CHEMISTRY OF MATERIALS

Article

pubs.acs.org/cm

Tailoring Physical Aging in Super Glassy Polymers with Functionalized Porous Aromatic Frameworks for CO_2 Capture

Cher Hon Lau,*[,†] Kristina Konstas,[†] Cara M. Doherty,[†] Shinji Kanehashi,[‡] Berkay Ozcelik,[‡,§] Sandra E. Kentish,[‡] Anita J. Hill,[†] and Matthew R. Hill*[,†]

[†]CSIRO Manufacturing Flagship, Private Bag 10, Clayton South, Melbourne, Victoria 3169, Australia

[‡]Department of Chemical and Biomolecular Engineering, The University of Melbourne, Melbourne, Victoria 3010, Australia

Supporting Information

ABSTRACT: A series of chemically functionalized porous aromatic frameworks (PAFs) have been synthesized and deployed within mixed-matrix membranes for gas separation. This series of PAFs delivered for the first time simultaneous control of selective gas transport and physical aging within the membranes. New composites including native and metalated fullerenes were also prepared, and the composites exhibited exceptional increases in their porosity, which in turn resulted in ultrafast gas transport. CO_2 permeability following PAF-1-Li_6C_{60} infusion within poly(trimethylsilylpropyne) was as high as 50 600 Barrer, a 70% improvement. Remarkably, just 9% of this permeation rate diminished after 1 year of physical aging, compared to 74% in the native polymer. A series of characterization techniques revealed this phenomenon to be due to intercalation of polymer chains within the PAF pores, the strength of which is controlled by the levels of chemical functionalization and porosity. The membranes were exploited for gas separations, in particular the stripping of CO_2 from natural gas.

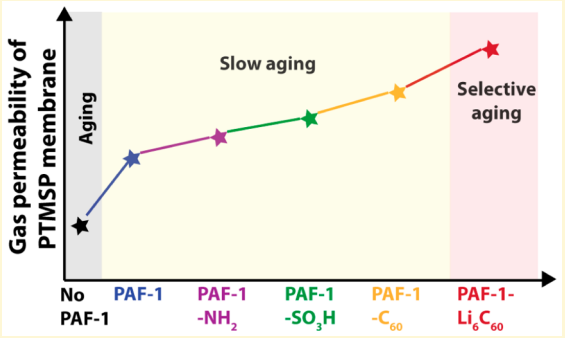

INTRODUCTION

Super glassy polymers age physically where the polymer main chains[1,2] converge and collapse the free volume content available for molecular transport. Attempts to address this have typically come at the detriment of other properties. Additives can drastically enhance gas permeability but do not restrain physical aging in super glassy polymers,[3−7] whereas polymer chain rigidification slows physical aging rates at the expense of permeability.[8] These are factors that inhibit the deployment of new polymers for membrane separations.[9,10]

The problem of physical aging remains an important issue to be fully resolved prior to exploiting super glass polymers such as the polyacetylene, poly(trimethylsilylpropyne) (PTMSP).[11] The ultrapermeability of PTMSP was first discovered in 1983 and was thought to be ideal for gas separation applications.[12] Inefficiently packed main PTMSP chains propped apart by the bulky trimethylsilyl side chains resulted in exceptionally high fractional free volume (FFV) content that induced superior gas permeability. However, it was soon realized that drastic reductions in PTMSP FFV content rendered them impractical for long-term separation applications. Ideal polymer separation membranes need to possess ultrapermeability while being immune to polymer aging.

We recently reported the inhibition of polymer aging in super glassy polymers like PTMSP without any gas permeability loss. In fact, gas permeabilities were enhanced.[13,14] This was achieved using finely dispersed additives (observed from microscopy images).[13] Such membranes were then deployed for H_2/N_2 separations and CO_2 separations. Among the different aging mechanisms observed across these works, the selective-aging mechanism was by far most interesting, as separation performances of such membranes bettered with age.

Porous aromatic frameworks (PAFs) are composed of polymerized tetraphenylmethane units and exhibit exceptionally high Brunauer−Emmett−Teller (BET) surface areas of any known material (i.e., 5600 m^2 g^{-1}).[15] PAFs are typically synthesized from quadricovalent monomers via a Yamamoto-type Ullmann cross-coupling reaction over metallic catalysts.[15] PAF surface area and CO_2 uptake can vary depending on the following characteristics: batch, tetrahedral core,[15,16] phenyl chain length, functionalization,[17−19] and also nanoparticle decoration.[20] The porosity and chemical functionality of PAF-1 nanoparticles can be engineered to suit application requirements.

Here, we demonstrate the effect of PAF-1 chemical functionality upon gas transport. There are significant effects upon gas permeability and physical aging rates that are linked to the chemical functionality and porosity of each PAF additive (Figure 1). Mixed gas permeations show that these mixed-matrix membranes are suitable as high flux gas separation membranes for CO_2 removal from flue gases and sweetening natural gas streams.

Received: April 24, 2015
Revised: June 17, 2015
Published: June 17, 2015

DOI: 10.1021/acs.chemmater.5b01537
Chem. Mater. 2015, 27, 4756−4762

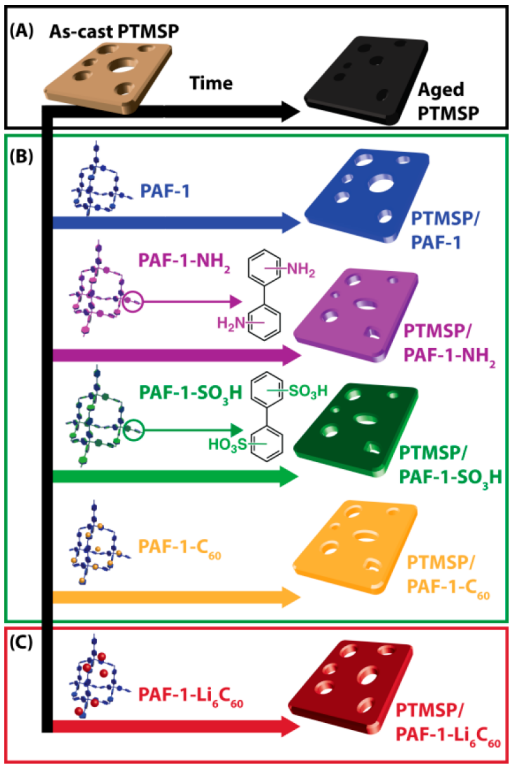

Figure 1. PTMSP membranes are prone to (a) physical aging (black), whereas (b) PTMSP membranes loaded with PAF-1 (blue), PAF-1-NH_2 (purple), PAF-1-SO3H (green), PAF-1-C_{60} (orange) show slow-aging properties; (c) PTMSP membranes loaded with PAF-1-Li_6C_{60} (red) display selective-aging properties.

EXPERIMENTAL SECTION

Materials Used. Polytrimethylsilylpropyne (PTMSP) was purchased from Gelest Inc. (Morrisville PA, U.S.A.) and used without purification. 1,5-Cyclooctadiene, bis(1,5-cyclooctadiene) nickel, 2,2′-bipyridyl, and tetrakis(4-bromophenyl) methane were purchased from Sigma-Aldrich. Tetrahydrofuran (THF), dry dimethylformamide (DMF), chloroform, dichloromethane (DCM), paraformaldehyde, diethylenetriamine (DETA), glacial acetic acid, chlorosulfonic acid (HSO_3Cl), phosphoric acid (H_3PO_4), and hydrochloric acid (HCl) were used as received.

PAF-1 Synthesis. PAF-1 was synthesized according to Zhu and co-workers to yield an off-white powder with a BET surface area of 3760 m^2/g.[15] 1,5-Cyclooctadiene (dried over CaH_2) was added into a solution of bis(1,5-cycloocatdiene) nickel and 2,2′-bipyridyl in dehydrated DMF. The mixture was heated for 1 h at 80 °C to form a purple solution. Tetrakis(4-bromophenyl)methane was added, and the mixture was stirred overnight at 80 °C. The mixture was allowed to cool to room temperature, and concentrated HCl was added. The solids were collected and washed with chloroform, THF, and deionized water. The particle size was typically in the range of 100–200 nm.

PAF-1 Functionalization. PAF-1 was aminated and sulfonated according to the approach of Zhou and co-workers.[17,18] Prior to amination, PAF-1 was chloromethylated. To chloromethylate PAF-1, paraformaldehyde, glacial acetic acid, H_3PO_4, and concentrated HCl were added to PAF-1 and stirred for 3 days at 90 °C. Subsequently, a light brown powder was collected after filtration and washing with deionized water. Chloromethylated PAF-1s were discharged into a stipulated amount of diethylenetriamine and stirred for 3 days at 90 °C. Aminated PAF-1 particles are known as PAF-1-NH_2 in this work. For sulfonation, PAF-1 was discharged into ice cold DCM, and HSO_3Cl was slowly added to the mixture and stirred for 3 days at ambient conditions. Thereafter, the mixture was poured into ice cold water, and a purple-blue powder was collected after washing with water. These particles are known as PAF-1-SO_3H in this work.

PAF-1 infiltrated with C_{60} nanoparticles or Li_6C_{60} composites were synthesized using a strategy outlined in Scheme 1. Briefly, dry PAF-1

Scheme 1. Infiltration of Li_6C_{60} into PAF-1 Nanoparticles

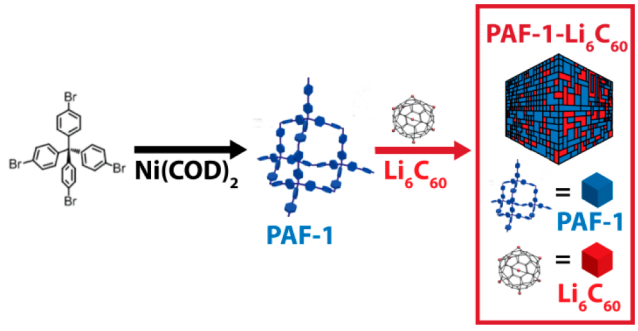

and freshly prepared C_{60} nanoparticles or Li_6C_{60} composites were placed in an inert environment. Loading was done between 5–20% of mass weight compared to the PAF. To this, freshly dried and distilled carbon disulfide solvent (30 mL) was added, and the reaction mixture was mechanically stirred overnight at room temperature. The solvent was removed by filtration, and the remaining material was subsequently washed and filtered with additional dry and distilled carbon disulfide solvent. These nanoparticles were used for membrane fabrication after gas adsorption experiments.

Membrane Fabrication. In the initial step, 8–10 wt % of PAF-1 (with respect of polymer concentration) was mixed with 2–5 wt % of PTMSP dissolved in chloroform or tetrahydrofuran (THF). The mixture was stirred for 24 h at ambient conditions, and ∼100 μm films were formed via solution casting at ambient conditions. The membrane films were dried in a vacuum oven at 60 °C for 24 h prior to gas permeability measurements. Film densities were measured using a helium pycnometer.

RESULTS AND DISCUSSION

1. PAF-1 Functionalization. PAF-1 was aminated and sulfonated according to the approach of Zhou and co-workers.[17,18] The BET surface areas (Table 1) of aminated

Table 1. BET Surface Area of PAF-1 and Its Functionalized Analogues

type of PAF-1	BET surface area (m^2/g)
PAF-1	3760
PAF-1-NH_2	879
PAF-1-SO_3H	829
PAF-1-C_{60}	3130
PAF-1-Li_6C_{60}	7360

and sulfonated PAF-1 nanoparticles were significantly lower than those of PAF-1, comparable to literature values.[17,18] The amine[18] and sulfonic acid[17] functional moieties filled up the pore volume of PAF-1, hence leading to lower BET surface areas.

PAF-1 samples infiltrated with C_{60} nanoparticles or Li_6C_{60} were synthesized using the strategy outlined in Scheme 1. Dry PAF-1 and freshly prepared C_{60} nanoparticles or Li_6C_{60} nanocomposites were placed in an inert environment. Loading was done between 5 and 20% of mass weight compared to the PAF. To this, freshly dried carbon disulfide solvent was added, and the reaction mixture was mechanically stirred overnight at room temperature. The solvent was removed by filtration, and

DOI: 10.1021/acs.chemmater.5b01537
Chem. Mater. 2015, 27, 4756–4762

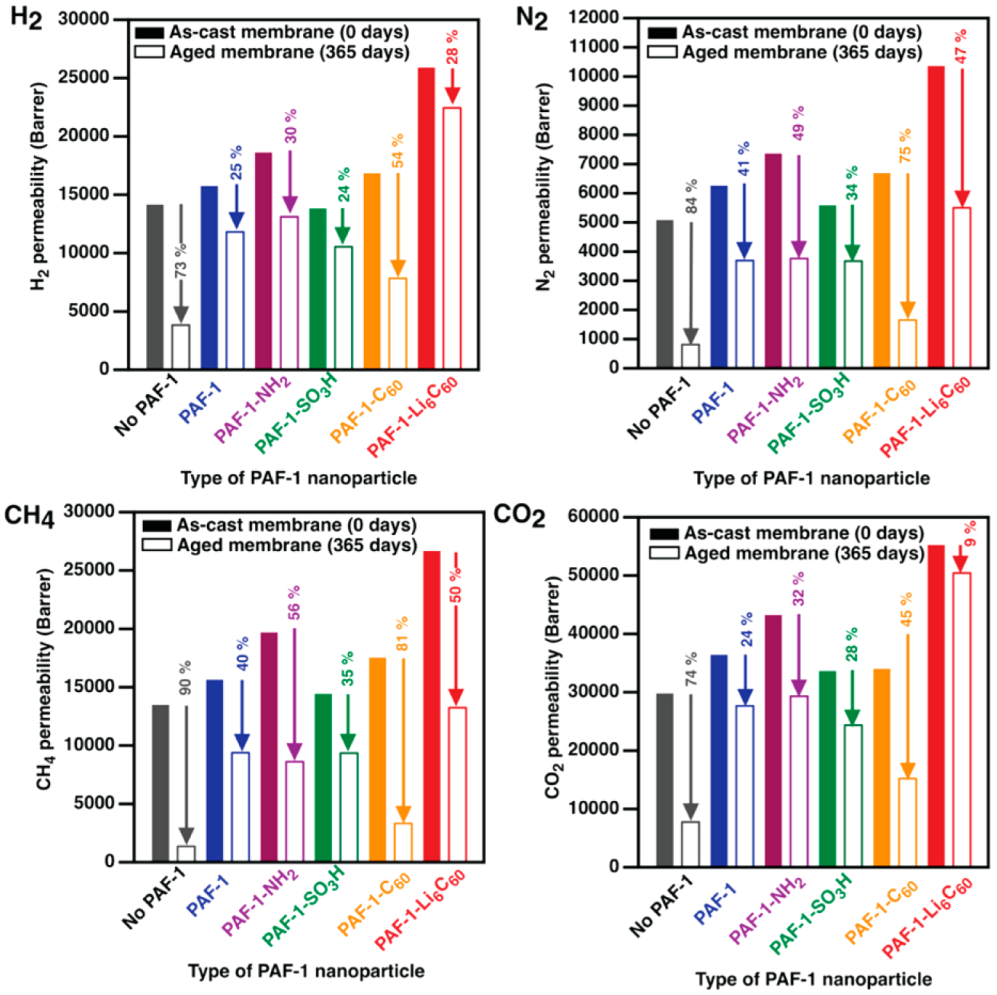

Figure 2. Gas permeabilities of PTMSP membranes loaded with 10 wt % of functionalized PAF-1 nanoparticles. The relative decrease in gas permeabilities (shown using arrows) between as-cast (filled bars) and aged (open bars) membranes are expressed in %. The standard deviation of gas permeabilities obtained from an average of three different films of similar thickness (130 ± 20 μm) is within ±10%.

the remaining material was subsequently washed and filtered with additional dry and distilled carbon disulfide solvent. These nanoparticles were used for membrane fabrication after gas adsorption experiments.

Similar to functionalized PAF-1, C_{60} incorporation partially filled PAF-1 pores, resulting in lower BET surface areas.[20] Meanwhile, the incorporation of Li_6C_{60} yielded PAF-1 with higher BET surface areas when compared to other functionalized PAF-1s studied in this work.

2. Effects of PAF-1 Functionalization on Physical Aging. Gas permeability measurements obtained from at least three different films of similar thicknesses (130 ± 20 μm) were used primarily to characterize physical aging in PTMSP/PAF nanocomposites. Amino and sulfonic acid moieties enhanced CO_2 uptake in PAF-1.[17,18] The BET surface areas of aminated and sulfonated PAF-1 nanoparticles were 76% lower than that of pristine PAF-1, yet CO_2 permeability enhancements in PTMSP/PAF-1-SO_3H and PTMSP/PAF-1-NH_2 were 10 and 15% larger than PTMSP/PAF-1 films (Figure 2). This highlighted the role of chemical interactions between polar $-NH_2$ and $-SO_3H$ functional moieties and CO_2 molecules; furthermore, it indicated the translation of favorable adsorption properties into the continuous membrane setting. PTMSP/PAF-1-NH_2 and PTMSP/PAF-1-SO_3H films aged slowly, where H_2, N_2, and CH_4 permeabilities were reduced by 30–70% over 365 days. Interestingly, CO_2 permeabilities of these films were only reduced by 20–50%. The preferential CO_2 transport in these membranes could be attributed to the enhanced affinity between the polar functional moieties and CO_2 molecules, similar to those observed in functionalized polymer membranes.[21,22]

PAF-1-Li_6C_{60} incorporation enhanced CO_2 permeabilities in PTMSP membranes by 85%, the largest enhancement observed in the present article. PTMSP/PAF-1-Li_6C_{60} films tested periodically exhibited selective-aging properties where H_2, N_2, and CH_4 permeabilities were reduced by 20–40% over 365 days, while maintaining CO_2 permeability. Additional CO_2 sorption sites from lithium atoms and the ultrahigh surface areas of PAF-1-Li_6C_{60} nanoparticles were responsible for the drastic CO_2 permeability enhancement and also the selective-aging mechanism observed here in this work.

The route to selective-aging membranes was achieved differently in our previous work, where pore size shrinkages in PIM-1/PAF-1 mixed-matrix membranes were tailored to accommodate all diffusion mechanisms of targeted gas molecules.[14] Presently, the dominant mechanism of selective-aging membranes was the enhanced gas sorption through additional adsorption sites, in the form of surface area and lithium atoms. CO_2 sorption experiments were performed on

DOI: 10.1021/acs.chemmater.5b01537
Chem. Mater. 2015, 27, 4756–4762

these membranes to quantify the amount of adsorbed CO_2 and were subsequently used to determine CO_2 diffusivity.

Gas sorption is governed by the affinity between the gas penetrant with chemical moieties, the polymer, and the concentration of sorption sites. The high surface areas of PAF-1 provided more exposed gas sorption sites that enhanced CO_2 uptake,[19] contributing to a 42% increment in CO_2 adsorption from 7.4 to 10.5 cm^3 STP/cm^{-3} atm in aged PTMSP/PAF-1 membranes (Table 2). Amine moieties

Table 2. CO_2 Permeability (P) [Barrer], Solubility ($\overline{S}$) [cm^3 STP/cm^{-3} atm], and Diffusivity ($\overline{D}$) [10^5 cm^2/s] Coefficients of Aged PTMSP-Based Membrane Films at 1 atm and 298 K

membrane	P_{CO_2}	$\overline{S}$	$\overline{D}$
PTMSP* (as-cast)	29 800	12.9	2.3
PTMSP	13 600	7.4	1.8
PTMSP/PAF-1	28 400	10.5	2.8
PTMSP/PAF-1-NH_2	35 100	10.7	4.3
PTMSP/PAF-1-SO_3H	32 400	10.4	3.1
PTMSP/PAF-1-C_{60}	25 800	13.7	2.1
PTMSP/PAF-1-Li_6C_{60}	50 600	18.6	2.7

exhibited physicochemical interactions with CO_2,[23] hence increasing the CO_2 solubility in PTMSP/PAF-1-NH_2 films by 45% to 10.7 cm^3 STP/cm^{-3} cmHg. PAF-1 sulfonation charged up the PAF-1 surface to impart strong affinity toward CO_2 via its quadrapole moment[17] and improved the CO_2 solubility in PTMSP/PAF-1-SO_3H films by 41% to 10.4 cm^3 STP/cm^{-3} atm. However, the advantage of enhancing CO_2 sorption through the interactions between polar functional groups and CO_2 molecules is offset through the much lower surface areas in functionalized PAF-1 nanoparticles. As the BET surface area of the PAF-1 additive increased from ~850 m^2/g (in amino and sulfonato PAF-1 nanoparticles) to 3130 m^2/g in PAF-1-C_{60}, the CO_2 sorption of resultant PTMSP-based membranes were enhanced by 85% to 13.7 cm^3 STP/cm^{-3} cmHg. Pseudo chemisorptive behavior between Li atoms and CO_2[19] in PAF-1-Li_6C_{60} led to large CO_2 uptakes, which consequently enhanced CO_2 sorption by 150% in PTMSP/PAF-1-Li_6C_{60} mixed-matrix membranes. Among postmodification techniques deployed in this work, Li_6C_{60}-decorated PAF-1 showed the strongest CO_2 affinity.

CO_2 diffusivity coefficients of aged PAF-1-based mixed-matrix membranes were larger than that of aged pristine PTMSP, and they were also crucial for enhancing CO_2 permeability. The larger diffusivity coefficients were intrinsically linked to the higher FFV content of PAF-1-based mixed-matrix membranes.

PALS analyses (Figure 3) were used to probe the pore sizes and concentrations present within the matrices. The bimodal pore size distribution of PTMSP observed here has been commonly reported in literature.[24−26] The large pore size distributions (centered at 15−16 Å) of aged membranes with PAF-1-NH_2, PAF-1-SO_3H, PAF-1-C_{60}, and PAF-1-Li_6C_{60} were wider, and these membranes had half the intensities of aged PTMSP/PAF-1 membranes centered at 15 Å. These enlarged large pore size distributions indicated PTMSP main chains were propped further apart by functionalized PAF-1, which were maintained even after 365 days of aging. This is similar to Hill's model where additional FFV content resulted from nanoparticle incorporation (Figure 3D).[27] This was crucial for maintaining enhanced gas permeabilities in our aged mixed-

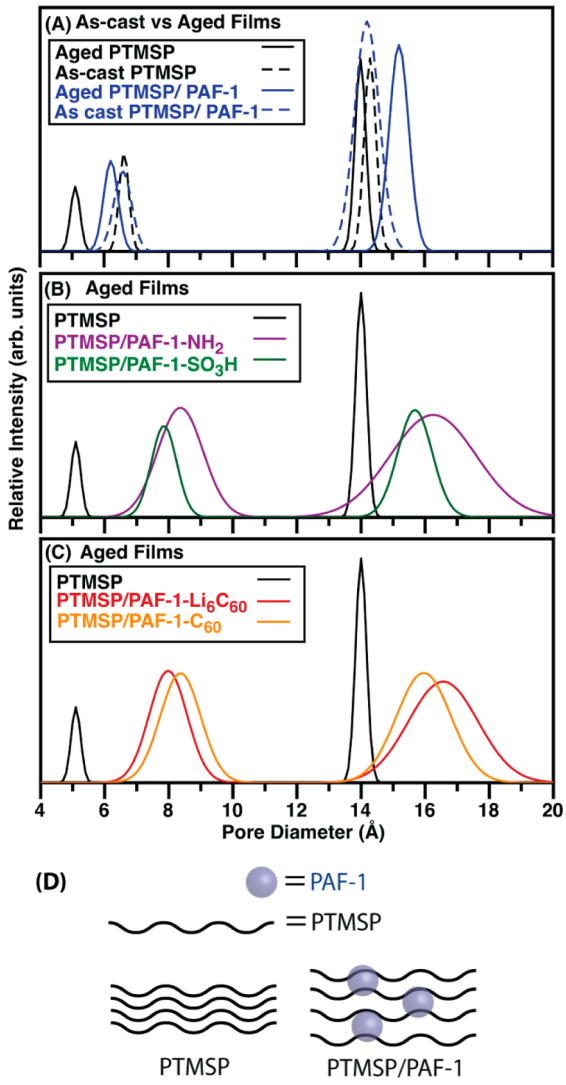

Figure 3. (A)−(C) Bulk PALS analyses showing the changes in pore size and concentration as a function of aging. (D) Cartoon depicting the propping apart of PTMSP chains.

matrix membranes. Considering that both PAF-1 and PTMSP possessed 12 Å pore size distributions,[13] their intensities would be higher if these materials did not intercalate or existed in different spatial domains. The lower intensities of 12 Å pore size distributions in aged PTMSP/PAF-based films indicated that PTMSP chains were well-intercalated within PAF-1 pores, hence pinpointing the location of physical interactions between the bulky side chains of PTMSP and the PAF-1 pores. This interaction was verified through ^{13}C solid-state NMR analyses.

T_1 relaxation times of carbon atoms derived from ^{13}C solid-state NMR were used to correlate mobilities of side and main chain carbons in PTMSP with polymer aging.[1,13,14,25] Increases in T_1 values have been correlated to lower mobility in carbon atoms, whereas reduced T_1 values indicate more mobile carbon atoms. The main chain carbon atom (b) of PTMSP became more mobile during aging as a result of being connected to the bulky trimethylsilyl side chains, which is the main driver for converging main chains (Figure 4).[25] The converged main chains collapsed FFV content, yielding less space for side chains to move. PAF-1 only impeded the mobility of main chain carbon (b) in PTMSP/PAF-1, whereas main chain carbon (c) continued to be mobile. The partial freedom of PTMSP chains

DOI: 10.1021/acs.chemmater.5b01537
Chem. Mater. 2015, 27, 4756−4762

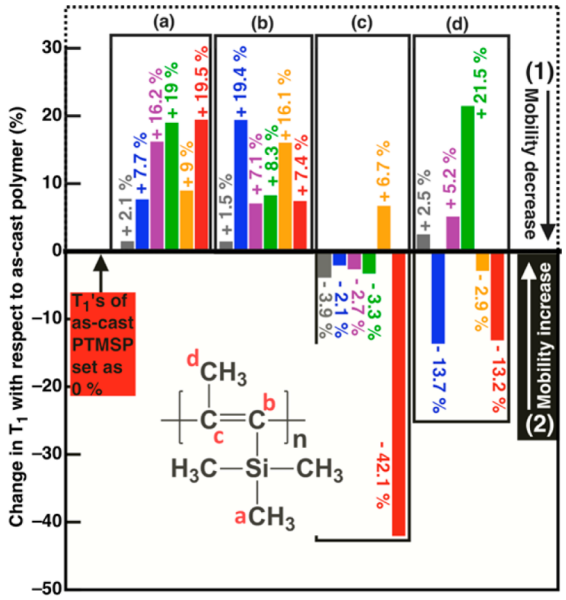

Figure 4. Comparison of carbon atom mobilities in the side chains, and main chains of PTMSP membranes loaded with different PAF-1 nanoparticles. T_1 relaxation times of as-cast PTMSP films were set as 0%. T_1 increments correlate to lower mobility in carbon atoms (1), whereas smaller T_1 values correspond to higher mobility in carbon atoms (2).

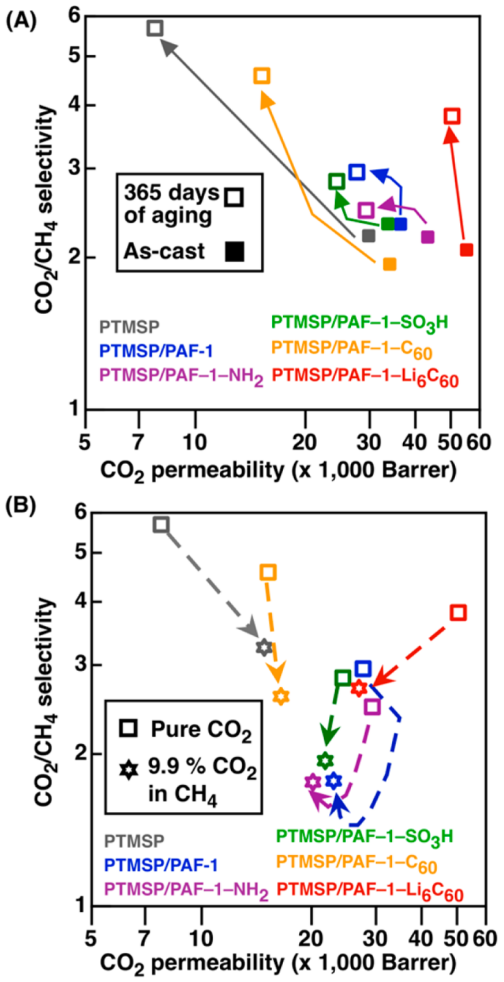

Figure 5. (A) CO_2/CH_4 pure gas permeabilities of membranes tracked over 365 days of physical aging and (B) a comparison of mixed and pure gas permeabilities of membranes physically aged for 365 days.

accounted for slow-aging properties, as the main chains continue to converge.

Compared to as-cast PTMSP, main chain carbons (b) and (c) in PTMSP membranes incorporated with amino and sulfonic acid functionalized PAF-1 were less mobile. These trends were also observed in mixed-matrix membranes loaded with PAF-1-C_{60} and PAF-1-Li_6C_{60}. The immobilization of main chain carbon atoms in PTMSP mixed-matrix membranes studied here was attributed to possible attractive forces between the polar functionalities with methyl groups in PTMSP,[28] as well as to $\pi-\pi$ interactions between aromatic rings of electron deficient C_{60} molecules and the unsaturated main chain carbon atoms.[29] The rigidification of main chain carbon atoms is the key to stopping and slowing PTMSP aging.

By incorporating functionalized PAF-1 into PTMSP, CO_2 permeabilities were enhanced, whereas CO_2/CH_4 selectivity remained largely similar (Figure 5). The CO_2/CH_4 selectivity of these membranes only increased after 365 days of aging, being caused by the drastic reductions in CH_4 permeability. This is also observed for CO_2/N_2 separations (Supporting Information). Additional CO_2 sorption sites and higher FFV content in these membranes could have further enhanced preferential CO_2 transport over CH_4 in the CH_4-majority gas we used in our experiments. PTMSP membranes loaded with functionalized PAF-1 rivaled as-cast membranes where handling and treatment of PTMSP mixed-matrix membranes has been optimized and yet remain prone to aging.[3−5,30,31] Coupled with the capability to mass-produce porous nanoparticles[32] and their selective-aging properties, these membranes are highly attractive for a range of separation challenges.

CONCLUSIONS

PAF-1 and its functionalized analogues were found to enhance gas permeabilities by at least 50% in mixed-matrix membranes. The high CO_2 affinity of PAF-1 benefitted CO_2 permeabilities of PTMSP membranes, with PTMSP/PAF-1-Li_6C_{60} membranes showing a 70% increment in CO_2 permeability from 29 800 Barrer to a remarkable 50 600 Barrer. Furthermore, incorporation of PAF-1, PAF-1-NH_2, PAF-1-SO_3H, and PAF-1-C_{60} drastically slowed physical aging in PTMSP membranes, whereas PAF-1-Li_6C_{60} maintained CO_2 permeability in PTMSP over 365 days concurrently with other gas permeabilities, delivering selective-aging membranes that improve with time. CO_2 sorption measurements revealed that the selective-aging mechanism in PTMSP/PAF-1-Li_6C_{60} membranes was caused by enhanced CO_2 sorption through additional adsorption sites, in the form of fractional free volume content and coordinatively unsaturated lithium atoms. Solid-state NMR spectroscopy elucidated the different rigidification degrees of PTMSP main chains by various functionalized PAF-1, which was the mechanism responsible for the slow and selective aging. This was exploited for the separation of CO_2 from natural gas, where performances were well above those typically obtained in polymer membranes.

ASSOCIATED CONTENT

Supporting Information

Details on PAF-1 synthesis and functionalization, membrane fabrication, CO_2 and N_2 adsorption isotherms, gas permeability and sorption measurements, bulk PALS experiments, and solid-

DOI: 10.1021/acs.chemmater.5b01537
Chem. Mater. 2015, 27, 4756−4762

state ^{13}C NMR. The Supporting Information is available free of charge on the ACS Publications website at DOI: 10.1021/acs.chemmater.5b01537.

AUTHOR INFORMATION

Corresponding Authors

*E-mail: cherhon.lau@csiro.au.
*E-mail: matthew.hill@csiro.au.

Present Address

[§]CSIRO Manufacturing Flagship, Private Bag 10, Clayton South, Melbourne, Victoria 3169, Australia

Author Contributions

The manuscript was written through contributions of all authors.

Funding

This work was supported by the Science and Industry Endowment Fund (SIEF). M.R.H. acknowledges FT1300345.

Notes

The authors declare no competing financial interest.

ACKNOWLEDGMENTS

The authors would like to thank Mr. Asoka Weerawardena for some single-gas permeation tests and Dr. Roger Mulder for solid-state NMR experiments.

REFERENCES

(1) Hill, A. J.; Pas, S. J.; Bastow, T. J.; Burgar, M. I.; Nagai, K.; Toy, L. G.; Freeman, B. D. Influence of Methanol Conditioning and Physical Aging on Carbon Spin-Lattice Relaxation Times of Poly(1-trimethylsilyl-1-propyne). *J. Membr. Sci.* **2004**, *243*, 37.

(2) Kurchan, J. In and Out of Equilibrium. *Nature* **2005**, *433*, 222.

(3) Matteucci, S.; Kusuma, V. A.; Sanders, D.; Swinnea, S.; Freeman, B. D. Gas Transport in TiO_2 Nanoparticle-filled Poly(1-trimethylsilyl-1-propyne). *J. Membr. Sci.* **2008**, *307*, 196.

(4) Matteucci, S.; Kusuma, V. A.; Kelman, S. D.; Freeman, B. D. Gas Transport Properties of MgO-filled Poly(1-trimethylsilyl-1-propyne) Nanocomposites. *Polymer* **2008**, *49*, 1659.

(5) De Sitter, K.; Winberg, P.; D'Haen, J.; Dotremont, C.; Leysen, R.; Martens, J. A.; Mullens, S.; Maurer, F. H. J.; Vankelecom, I. F. J. Silica Filled Poly(1-trimethylsilyl-1-propyne) Nanocomposite Membranes: Relation Between the Transport of Gases and Structural Characteristics. *J. Membr. Sci.* **2006**, *278*, 83.

(6) De Sitter, K.; Andersson, A.; D'Haen, J.; Leysen, R.; Mullens, S.; Maurer, F. H. J.; Vankelecom, I. F. J. Silica filled Poly(4-methyl-2-pentyne) Nanocomposite Membranes: Similarities and Differences with Poly(1-trimethylsilyl-1-propyne)−Silica Systems. *J. Membr. Sci.* **2008**, *321*, 284.

(7) Smith, S. J. D.; Ladewig, B. P.; Hill, A. J.; Lau, C. H.; Hill, M. R. H. Ti-Loaded Metal-Organic Frameworks that Deliver Exceptional Gas Permeability in Mixed Matrix Membranes. *Sci. Rep.* **2014**, *5*, 7823.

(8) Shao, L.; Samseth, J.; Hägg, M.-B. Effect of Plasma Treatment on the Gas Permeability of Poly(4-methyl-2-pentyne) Membranes. *Plasma Process Polym.* **2007**, *4*, 823.

(9) Staiger, C. L.; Pas, S. J.; Hill, A. J.; Cornelius, C. J. Free Volume Distribution, and Physical Aging of a Highly Microporous Spirobisindane Polymer. *Chem. Mater.* **2008**, *20*, 2606.

(10) Rowe, B. W.; Freeman, B. D.; Paul, D. R. Physical Aging of Ultrathin Glassy Polymer Films Tracked by Gas Permeability. *Polymer* **2009**, *50*, 5565.

(11) Nagai, K.; Masuda, T.; Nakagawa, T.; Freeman, B. D.; Pinnau, I. Poly[1-(trimethylsilyl)-1-propyne] and Related Polymers: Synthesis, Properties and Functions. *Prog. Polym. Sci.* **2001**, *26*, 721.

(12) Masuda, T.; Isobe, E.; Higashimura, T.; Takada, K. Poly[1-(trimethylsilyl)-1-propyne]: A New High Polymer Synthesized with Transition-Metal Catalysts and Characterized by Extremely High Gas Permeability. *J. Am. Chem. Soc.* **1983**, *105*, 7473.

(13) Lau, C. H.; Nguyen, P. T.; Hill, M. R.; Thornton, A. W.; Konstas, K.; Doherty, C. M.; Mulder, R. J.; Bourgeois, L.; Liu, A. C. Y.; Sprouster, D. J.; Sullivan, J. P.; Bastow, T. J.; Hill, A. J.; Gin, D. L.; Noble, R. D. Ending Aging in Super Glassy Polymer Membranes. *Angew. Chem., Int. Ed.* **2014**, *53*, 5322.

(14) Lau, C. H.; Konstas, K.; Thornton, A. W.; Liu, A. C. Y.; Mudie, S. T.; Kennedy, D. F.; Howard, S. C.; Hill, A. J.; Hill, M. R. Porous Aromatic Framework-Loaded Gas Separation Membranes that Improve with Age. *Angew. Chem., Int. Ed.* **2015**, *54*, 2669.

(15) Ben, T.; Ren, H.; Ma, S.; Cao, D.; Lan, J.; Jing, X.; Wang, W.; Xu, J.; Deng, F.; Simmons, J. M.; Qiu, S.; Zhu, G. Targeted Synthesis of a Porous Aromatic Framework with High Stability and Exceptionally High Surface Area. *Angew. Chem.* **2009**, *121*, 9621.

(16) Yuan, D.; Lu, W.; Zhao, D.; Zhou, H.-C. Highly Stable Porous Polymer Networks with Exceptionally High Gas-Uptake Capacities. *Adv. Mater.* **2011**, *23*, 3723.

(17) Lu, W.; Yuan, D.; Sculley, J.; Zhao, D.; Krishna, R.; Zhou, H.-C. Sulfonate-Grafted Porous Polymer Networks for Preferential CO_2 Adsorption at Low Pressure. *J. Am. Chem. Soc.* **2011**, *133*, 18126.

(18) Lu, W.; Sculley, J. P.; Yuan, D.; Krishna, R.; Wei, Z.; Zhou, H.-C. Polyamine-Tethered Porous Polymer Networks for Carbon Dioxide Capture from Flue Gas. *Angew. Chem., Int. Ed.* **2012**, *51*, 7480.

(19) Konstas, K.; Taylor, J. W.; Thornton, A. W.; Doherty, C. M.; Lim, W. X.; Bastow, T. J.; Kennedy, D. F.; Wood, C. D.; Cox, B. J.; Hill, J. M.; Hill, A. J.; Hill, M. R. Lithiated Porous Aromatic Frameworks with Exceptional Gas Storage Capacity. *Angew. Chem., Int. Ed.* **2012**, *51*, 6639.

(20) Thornton, A. W.; Nairn, K. M.; Hill, J. M.; Hill, A. J.; Hill, M. R. Metal−Organic Frameworks Impregnated with Magnesium-Decorated Fullerenes for Methane and Hydrogen Storage. *J. Am. Chem. Soc.* **2009**, *131*, 10662.

(21) Mason, C. R.; Maynard-Atem, L.; Heard, K. W. J.; Satilmis, B.; Budd, P. M.; Friess, K.; Lanč, M.; Bernardo, P.; Clarizia, G.; Jansen, J. C. Enhancement of CO_2 Affinity in a Polymer of Intrinsic Microporosity by Amine Modification. *Macromolecules* **2014**, *47*, 1021.

(22) Khan, A. L.; Li, X.; Vankelecom, I. F. J. Mixed-Gas CO_2/CH_4 and CO_2/N_2 Separation with Sulfonated PEEK Membranes. *J. Membr. Sci.* **2011**, *372*, 87.

(23) Wang, H.; Paul, D. R.; Chung, T.-S. Surface Modification of Polyimide Membranes by Diethylenetriamine (DETA) Vapor for H_2 Purification and Moisture Effect on Gas Permeation. *J. Membr. Sci.* **2013**, *430*, 223.

(24) Consolati, G.; Genco, I.; Pegoraro, M.; Zanderighi, L. Positron Annihilation Lifetime (PAL) in Poly[1-(trimethyl-silyl)propine] (PTMSP): Free Volume Determination and Time Dependence of Permeability. *J. Polym. Sci., Part B: Polym. Phys.* **1996**, *34*, 357.

(25) Nagai, K.; Freeman, B. D.; Hill, A. J. Effect of Physical Aging of Poly(1-trimethylsilyl-1-propyne) Films Synthesized with $TaCl_5$ and $NbCl_5$ on Gas Permeability, Fractional Free Volume, and Positron Annihilation Lifetime Spectroscopy Parameters. *J. Polym. Sci., Part B: Polym. Phys.* **2000**, *38*, 1222.

(26) Yampol'skii, Y. P.; Shantorovich, V. P.; Chernyakovskii, F. P.; Kornilov, A. I.; Plate, N. A. Estimation of Free Volume in Poly(trimethylsilyl propyne) by Positron Annihilation and Electrochromism Methods. *J. Appl. Polym. Sci.* **1993**, *47*, 85.

(27) Hill, R. J. Reverse-Selective Diffusion in Nanocomposite Membranes. *Phys. Rev. Lett.* **2006**, *96*, 216001.

(28) Cong, H.; Radosz, M.; Towler, B. F.; Shen, Y. Polymer−Inorganic Nanocomposite Membranes for Gas Separation. *Sep. Purif. Technol.* **2007**, *55*, 281.

(29) Suezawa, H.; Yoshida, T.; Ishihara, S.; Umezawa, Y.; Nishio, M. CH/[π] Interactions as Disclosed on the Fullerene Convex Surface. *CrystEngComm* **2003**, *5*, 514.

(30) Shao, L.; Samseth, J.; Hägg, M.-B. Crosslinking and Stabilization of Nanoparticle Filled Poly(1-trimethylsilyl-1-propyne) Nanocomposite Membranes for Gas Separations. *J. Appl. Polym. Sci.* **2009**, *113*, 3078.

DOI: 10.1021/acs.chemmater.5b01537
Chem. Mater. 2015, 27, 4756−4762

(31) Merkel, T. C.; He, Z.; Pinnau, I.; Freeman, B. D.; Meakin, P.; Hill, A. J. Effect of Nanoparticles on Gas Sorption and Transport in Poly(1-trimethylsilyl-1-propyne). *Macromolecules* **2003**, *36*, 6844.
(32) Rubio-Martinez, M.; Batten, M. P.; Polyzos, A.; Carey, K.-C.; Mardel, J. I.; Lim, K.-S.; Hill, M. R. Versatile, High Quality and Scalable Continuous Flow Production of Metal-Organic Frameworks. *Sci. Rep.* **2014**, *4*, 5443.

DOI: 10.1021/acs.chemmater.5b01537
Chem. Mater. 2015, 27, 4756−4762